Synaptotagmin-13 Is a Neuroendocrine Marker

Subjects: Cell Biology

Contributor: Mostafa Bakhti

Synaptotagmin-13 (Syt13) is an atypical member of the vesicle trafficking synaptotagmin protein family. The expression pattern and the biological function of this Ca2+-independent protein are not well resolved. Here, we have generated a novel Syt13-Venus fusion (Syt13-VF) fluorescence reporter allele to track and isolate tissues and cells expressing Syt13 protein. The reporter allele is regulated by endogenous cis-regulatory elements of Syt13 and the fusion protein follows an identical expression pattern of the endogenous Syt13 protein. The homozygous reporter mice are viable and fertile.

Keywords: synaptotagmin-13 ; Syt13 ; fluorescent reporter

1. Introduction

Synaptotagmins (SYTs) are membrane trafficking proteins that regulate intracellular vesicle movement and exocytosis. In mammals, this protein family comprises 17 isoforms that are structurally characterized by an extracellular N-terminus region, a transmembrane (TM) domain and two tandem cytoplasmic (C2) domains at the C-terminus [1][2][3]. In several isoforms such as Syt1, Syt2, and Syt7, the C2 domains harbor Ca^{2+}-interacting residues and their function requires Ca^{2+}-binding [4][5][6][7]. SYTs are mainly expressed in neurons and cell types that possess regulatory secretory pathways. Among these are neuroendocrine cells, which produce and secrete hormones into the blood circulation to regulate different systematic processes such as metabolism [8][9]. The typical Ca^{2+}-dependent members such as Syt1 and Syt2 are well-known to mediate synaptic vesicle exocytosis. These proteins bind to the soluble NSF attachment protein receptor (SNARE) proteins and mediate vesicle docking and fusion to the target membranes [2]. Several other SYT isoforms such as Syt4, Syt8, and Syt13 lack the Ca^{2+}-binding amino acids and operate in a Ca^{2+}-independent manner [7][10]. These Ca^{2+}-independent atypical members are less functionally characterized [9].

Syt13 is an atypical SYT protein, which lacks an extracellular N-terminus sequence and is evolutionarily conserved with a high degree of homology between human and rodent sequences [11][12]. Syt13 mRNA is expressed in the brain, heart, lung, testis, spleen, kidney and pancreas [11][12][13]. An increase in the mRNA levels of Syt13 in several brain regions after contextual fear conditioning has been shown [14]. Moreover, Syt13 plays a protective function in motor neurons of patients with amyotrophic lateral sclerosis (ALS) and spinal muscular atrophy (SMA) [15]. Further, SYT13 is upregulated in several cancer cell types, such as gastric and colorectal cancers as well as lung adenocarcinoma.

2. Generation of the Syt13-Venus Fusion Mouse Line

To provide a reliable and efficient tool for tracking and isolating cells expressing Syt13 protein, we applied CRISPR/Cas9-mediated double strand breaks and homologous recombination to generate a mouse line, in which Syt13 is fused with the fluorescence protein Venus. We generated a Syt13-Venus fusion (Syt13-VF) reporter allele under control of the endogenous Syt13 cis-regulatory elements (**Figure 1**A). To do this, we removed the translational stop codon of the Syt13 gene in exon 6 and inserted an in-frame fusion transcript of the Venus open-reading frame. Additionally, we used an FRT-flanked phospho-glycerate kinase (PGK) promoter-driven neomycin (neo) resistance gene as the selection marker. The targeting vector, Cas9D10A expression vector, and two guide RNA vectors expressing guide RNAs that bind shortly before and after the Syt13 stop codon were electroporated into IDG3.2 embryonic stem cells (ESCs) [16]. Neomycin resistant clones were screened with 5′ and 3′ homology arm spanning PCRs (**Figure 1**B,C). Germline chimeras of the Syt13-VFneo mouse line were generated from the aggregation of Syt13-VFneo mESC clone with CD1 morulae. The FRT-flanked neo selection cassette was deleted in the germline by Flpe recombination-mediated excision [17] (**Figure 1**D), resulting in generation of the Syt13-VF mouse line. The intercross of heterozygous animals ($Syt13^{+/VF}$) produced wild-type (WT, $Syt13^{+/+}$), heterozygous and homozygous ($Syt13^{VF/VF}$) offspring that were genotyped by PCR analysis (**Figure 1**E). $Syt13^{VF/VF}$ offspring were viable and fertile and appeared indistinguishable from their WT or heterozygous adult littermates (**Figure 1**F). A 17-month close observation showed no postnatal death, as well as normal sociability, behavior, and health of the reporter mice (132 total animals). The average weight of 6-month-old male mice was 31 g for WT and 32

g for homozygous reporter animals (n = 8). The average number of animals per litter in heterozygous intercrosses was 5.75 (n = 8), and for homozygous intercrosses it was 5.52 (n = 23). Together, these data indicate the successful generation of Syt13-VF allele and the reporter mouse line. To disclose the target tissues for the expression pattern analysis of Syt13-VF protein, we next performed reverse transcription PCR (RT-PCR) of different organ samples isolated from the adult WT mice to identify the expression pattern of Syt13 mRNA. Syt13 was expressed in the brain (forebrain, cerebellum, brainstem, and pituitary), lung, pancreas, liver, kidney, intestine (duodenum, ileum, jejunum, and colon) and muscle (**Figure 1**G), confirming the broad expression of this gene as has been shown previously [11][12][13].

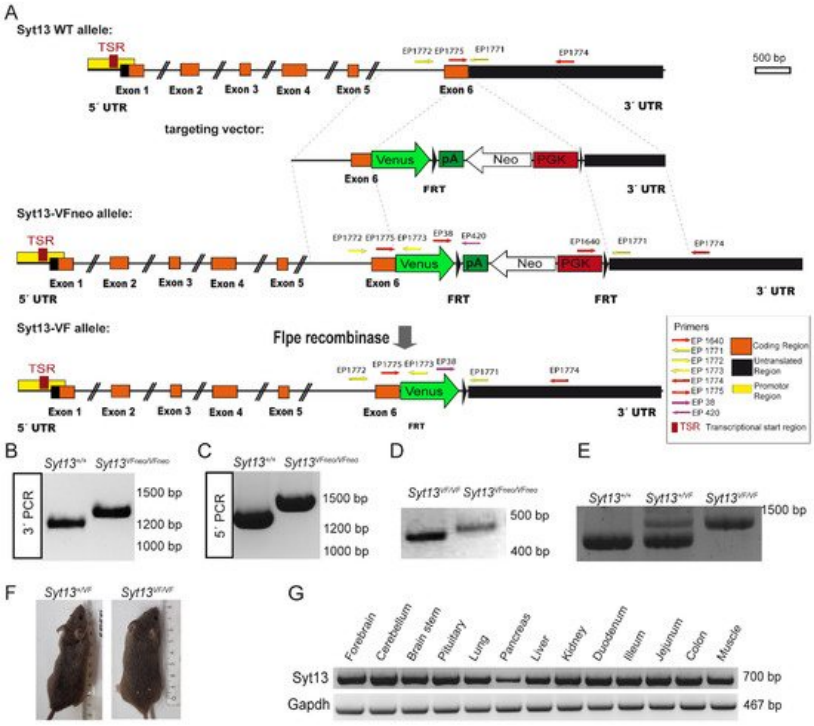

Figure 1. Generation of the Syt13 Venus Fusion (Syt13-VF) allele. (**A**) Targeting strategy of the Syt13-VF allele. A double strand break was performed by two nickases of the D10A mutant Cas9 using two gRNAs binding before and after the stop codon of Syt13. A targeting vector was used to repair the gap and fuse the coding region of the fluorescent reporter gene Venus to the open reading frame. The FRT-flanked PGK-driven neomycin (Neo) selection cassette was removed by Flpe recombinase-mediated excision. Syt13 5′ and 3′ untranslated regions (UTRs) are indicated in black and the predicted promoter region in yellow and the transcriptional start sites (TSR) in red as indicated. Primers used for genotyping EP_1771, EP_1772 and EP_1773 are indicated with yellow arrows. The position of the homology regions to generate the targeting construct are indicated (dashed lines). (**B**,**C**) PCR genotyping of Syt13VFNeo clones using primers EP_1640, EP_1774 and EP1775 (red arrows) confirming the targeted allele Syt13-VFNeo (1335 bp) versus the WT allele (1228 bp) and for 3′PCR and EP_1771, EP_1772, and EP_1773 for 5′PCR (yellow arrows) confirmation of Syt13-VFNeo (1475 bp) versus WT allele (1322 bp). (**D**) PCR primers EP038, EP420, and EP 1771 were used to distinguish the allele before (Syt13-VFNeo; 477 bp) and after removal of the Neo selection cassette (Syt13-VF; 402 bp). (**E**) Primers EP_1771, EP_1772, and EP_1773 were used to distinguish WT from heterozygous or homozygous mice resulting in 1322 bp for the WT allele and 1475 bp for the Syt13-VF allele. (**F**) Side by side image of a WT male mice (left) and a Syt13-VF male mouse (right) of 5 months of age. (**G**) RT-PCR of different tissues of a WT adult mouse presenting bands corresponding to Syt13 and Gapdh transcripts.

3. Syt13 Is Highly Expressed in Neuroendocrine Cells

To identify the expression pattern of Syt13 in the brain, we first performed quantitative PCR (qPCR) analysis. We detected Syt13 transcripts with high levels in forebrain and cerebellum, and with lower levels in brainstem and pituitary (**Figure 2**A). Furthermore, authors performed immunohistochemical (IHC) analysis of brain sections from Syt13$^{VF/VF}$ mice. Although it was possible to detect the fluorescent signal in the Venus-expressing cells, authors used antibodies against Venus protein to amplify the signal, showing the expression of Syt13-VF protein in the cortex, cerebellum, midbrain, hypothalamus, hippocampus, and medulla (**Figure 2**B). Although the IHC showed variable levels of Syt13-VF in different brain area, further studies are required to quantitatively validate this differential expression levels of Syt13. These data also support a previous study, which has reported a broad expression of Syt13 in several areas of the brain using in situ hybridization [18]. Importantly, co-staining of brain sections with antibodies against Syt13 and Venus disclosed high overlap between the two proteins (**Figure 2**C). This result indicates that the fusion protein accurately mirrors the expression of the endogenous

Syt13 protein. We next explored the expression pattern of Syt13 in different brain cell types. qPCR analysis revealed the expression of Syt13 mRNA in isolated neurons but not in microglia and astrocytes (**Figure 2**D). Furthermore, IHC of brain sections from Syt13$^{VF/VF}$ mice also revealed the expression of Syt13-VF protein in neurons (marked with NeuroTraceTM) [19] but not in microglia (marked with ionized calcium binding adaptor molecule 1, Iba1) or in astrocytes (marked with glial fibrillary acidic protein, GFAP) (**Figure 2**E–G). As most SYT members are expressed in neuroendocrine cells, we thus co-stained Venus and neuroendocrine specific markers. Authors found colocalization of Venus with tyrosine hydroxylase (TH)-expressing and oxytocin-producing cells (**Figure 2**H,I). These data indicate the high expression of Syt13 in neuroendocrine lineage as it has been reported for several other SYT proteins. However, the precise expression pattern of Syt13 protein in other neuronal cell types need to be further demonstrated in future studies.

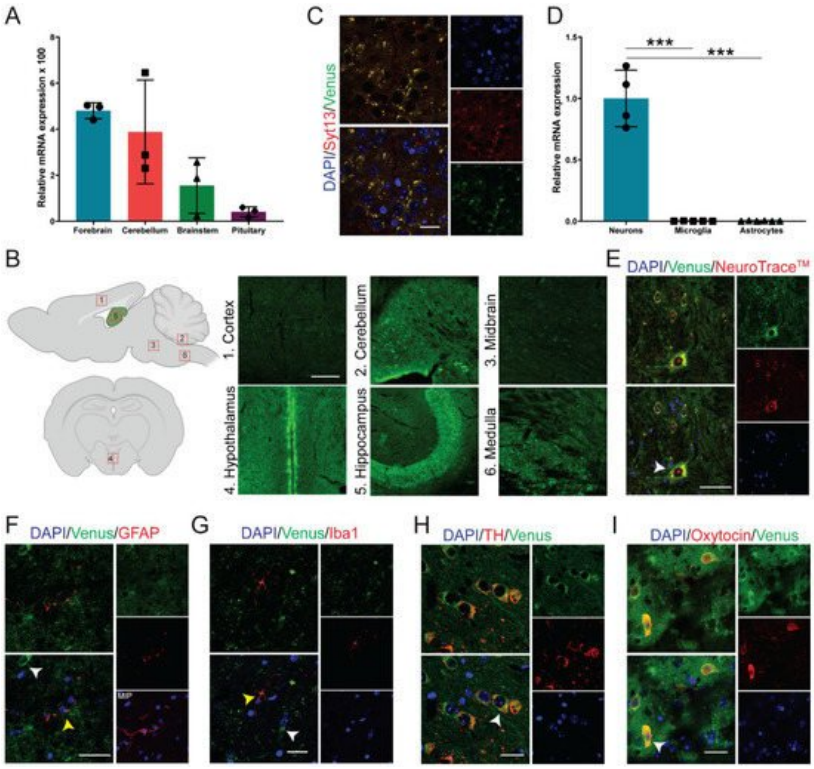

Figure 2. Syt13-VF expression in neuronal tissue. (**A**) Syt13 mRNA expression in different brain regions of adult WT male mice (n = 3). Transcript levels were calculated according to the $2^{-\Delta Ct}$ method; Gapdh was used as endogenous control to normalize mRNA amount. Bars represent means $2^{-\Delta Ct} \times 100 \pm$ SD. (**B**) Scheme of brain area used for IHC, and maximum intensity projection images of Syt13-VF positive cells at different brain regions including cortex, between IV-VI cortex layers; cerebellum, an area in the proximity of the interposed cerebellar nucleus (anterior part to posterior part) and the medial (fastigial) cerebellar nucleus; midbrain, an area in the proximity of the paramedian raphe nucleus and the pontine reticular nucleus; hypothalamus (coronal orientation), anterior hypothalamus in the 3V proximity; hippocampus, CA2 region area; medulla (sagittal orientation), inferior olive area. Scale bar 100 µm. Scheme was created with BioRender.com (accessed on May 2021). (**C**) Co-staining of GFP and Syt13 in the brain cortex shows co-localization of both markers. Scale bar 20 µm. (**D**) Analysis of Syt13 mRNA expression in neuron and glia cells isolated from WT animals shows high expression of Syt13 in neurons but not in microglia nor astrocytes ($n \geq 4$). (**E**–**G**) Immunostaining of brain sections confirm the presence of the Syt13-VF protein in neurons marked by NeuroTraceTM, but not in microglia or astrocytes marked by Iba1 and GFAP, respectively. White arrows indicate Syt13-VF and yellow arrows show glia cells. MIP, maximum intensity projection. Scale bar 20 µm. (**H**,**I**) Immunostaining analysis of hypothalamus regions showing colocalization of Syt13-VF with tyrosine hydroxylase (TH) and oxytocin, markers of neuroendocrine cells (white arrows). Scale bar 20 µm. (*** $p <$ 0.001; t-test). For (**E**–**I**), single confocal images were used to avoid false colocalization. Data are represented as mean ± SD.

4. Syt13 Expression Is Restricted to Enteroendocrine Cells in the Adult Intestine

RT-PCR data indicated the expression of Syt13 mRNA in several intestinal areas (**Figure 1**G). To support these data and identify the expression of Syt13 protein in this organ, we stained intestinal sections from the reporter mice with antibodies against Syt13 and Venus. We detected highly overlapping signals for both antibodies (**Figure 3**A,B) that not only indicates the expression of Syt13 proteins in the intestine but further confirms the identical expression pattern of the Syt13-VF proteins and endogenous Syt13 in this organ. To dissect in which intestinal cell types Syt13 is mainly expressed, we first

reanalyzed the single-cell RNA sequencing (scRNA-seq) data derived from mouse intestinal crypts [20]. Data analysis indicated the expression of Syt13 in all enteroendocrine cells (EECs) and a major fraction of their progenitors but no other intestinal cell types (**Figure 3**C–E). To confirm these data, we stained intestinal sections from Syt13$^{VF/VF}$ mice for Venus and markers for different intestinal cell types. We found the colocalization of Venus with the EEC marker, Chromogranin A (ChgA) (**Figure 3**F). However, no colocalization was found with lysozyme 1 (Lys1) (Paneth cells), Mucin 2 (Muc2) (Goblet cells), and Vimentin (Mesenchyme) (**Figure 3**G–I), demonstrating the restricted expression of Syt13 to the EEC and their progenitors in the intestine. Finally, we executed live imaging of isolated crypts derived from Syt13$^{VF/VF}$ mice. Due to the sufficient fluorescent intensity of the Syt13-VF reporter, we were able to track Syt13 expressing-cells during time-lapse imaging (**Figure 3**J).

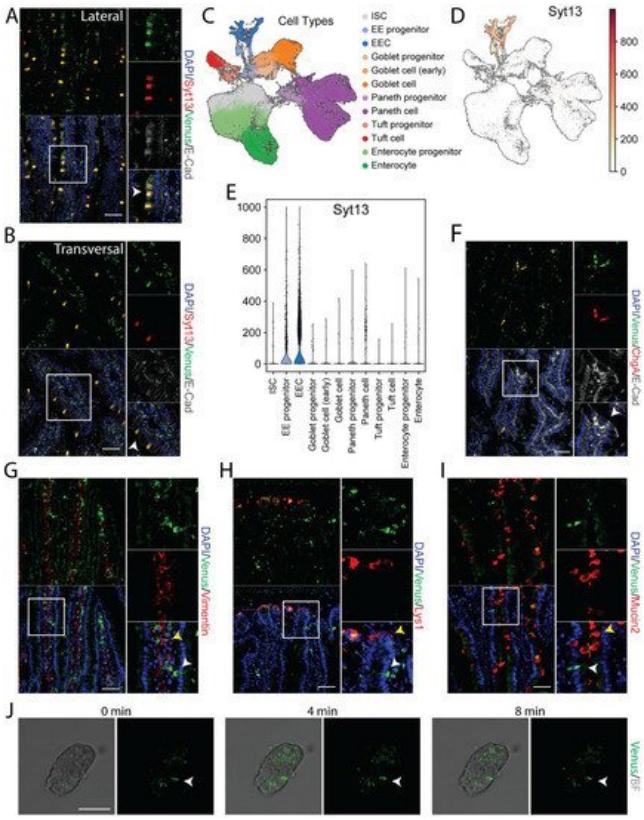

Figure 3. Syt13-VF expression in the adult intestinal epithelium. (**A**,**B**) Co-staining of GFP and Syt13 in intestinal villi from duodenum prepared from the reporter mice. Both markers show co-localization (white arrows) in the lateral and transversal cut. Scale bar 20 µm. (**C**) UMAP plot of 56240 profiled single cells from control mice. Colors highlight clustering into the main cell types and their progenitors. (**D**) Syt13 expression and distribution in UMAP plot. Normalized expression values are shown. (**E**) Violin plot of normalized expression of Syt13 grouped by cell type, showing the highest expression values in enteroendocrine progenitor cells (EE progenitor) and mature enteroendocrine cells (EEC). (**F**) Immunostaining analysis of Syt13-VF and chromogranin A (ChgA) shows colocalization (white arrows) of both markers. Scale bar 20 µm. (**G**–**I**) Syt13-VF does not colocalized with markers for paneth cells, goblet cells, and mesenchymal cells. White arrows indicate Syt13-VF and yellow arrows show cell types. Scale bar 20 µm. (**J**) Time-lapse imaging of an isolated crypt from Syt13-VF reporter mice. White arrows indicate Syt13-VF-expressing cell. Scale bar 50 µm. BF, bright field.

5. Pancreatic Endocrine but Not Exocrine Cells Specifically Express Syt13 Protein

Several SYT proteins such as Syt4 and Syt7 are expressed in pancreatic endocrine cells [21][22]. Moreover, islets of Langerhans from patients with type 2 diabetes contain decreased expression levels of Syt13 mRNA [23]. Therefore, we next assessed the expression pattern of Syt13-VF protein in the adult pancreas. Staining of pancreatic sections from Syt13$^{VF/VF}$ mice identified co-expression of Venus with the endocrine lineage marker, ChgA (**Figure 4**A). Yet, no specific signal for Venus was detected in amylase-expressing acinar cells (**Figure 4**B). These data suggest restricted expression of Syt13 to the pancreatic endocrine cells. Next, we performed fluorescence-activated cell sorting (FACS) to specifically isolate Syt13-VF-expressing cells. To this end, we performed FACS sorting on a mixture of islets and exocrine tissues (acinar and ductal cells) isolated from the adult pancreas from Syt13$^{VF/VF}$ mice. The bright fluorescence of Venus was sufficient for the successful segregation and isolation of Syt13-VF-positive (pos) and Syt13-VF-negative (neg) cell populations (**Figure 4**C). We then performed qPCR analysis of the harvested cells and confirmed the expression of both

Syt13 and Venus in the Syt13-VF^{pos} population, indicating the capability of the fusion reporter protein for specific isolation of Syt13-expressing cells (**Figure 4**D). Further, we identified the high expression levels of ChgA and amylase in the Syt13-VF^{pos} and Syt13-VF^{neg} cells, respectively (**Figure 4**E), indicating the specific expression of Syt13-VF in the pancreatic endocrine lineage.

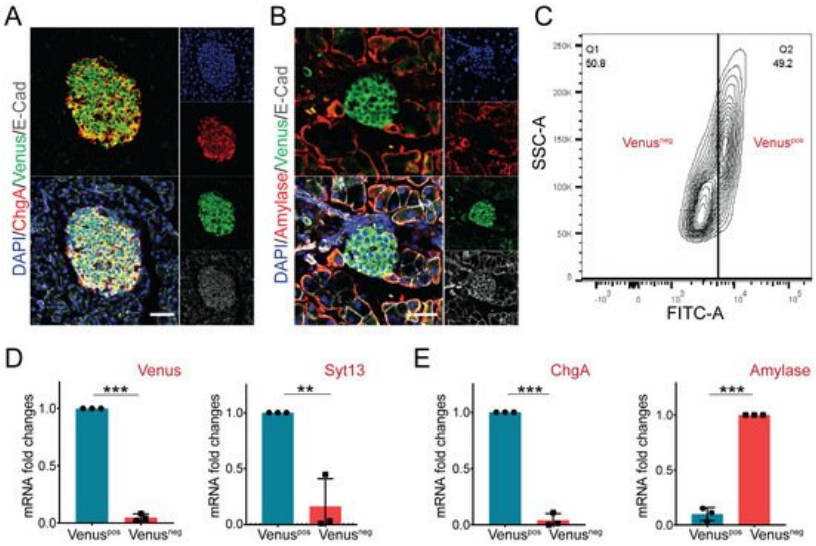

Figure 4. Syt13-VF expression in the adult pancreatic cells. (**A**) Immunostaining analysis of Syt13-VF expression in ChgA-expressing islet cells in pancreatic sections prepared from the reporter mice. Scale bar 20 µm. (**B**) No colocalization between Syt13-VF and amylase-expressing cells is detected. Scale bar 20 µm. (**C**) Representative FACS plot indicating the successful separation of Venus-positive (Venus^{pos}) cells from Venus-negative (Venus^{neg}) cells. (**D**) qPCR analysis shows high expression levels of Venus and Syt13 in Venus^{pos} cells isolated by FACS (n = 3). (**E**) qPCR analysis indicated high expression levels of ChgA and amylase in Venus^{pos} and Venus^{neg} cells, respectively (n = 3). (** $p < 0.01$;*** $p < 0.001$; t-test). Data are represented as mean ± SD.

References

1. Südhof, T.C. Synaptotagmins: Why so many? J. Biol. Chem. 2002, 277, 7629–7632.
2. Rickman, C.; Craxton, M.; Osborne, S.; Davletov, B. Comparative analysis of tandem C2 domains from the mammalian synaptotagmin family. Biochem. J. 2004, 378, 681–686.
3. Dai, H.; Shin, O.H.; Machius, M.; Tomchick, D.R.; Südhof, T.C.; Rizo, J. Structural basis for the evolutionary inactivation of Ca2+ binding to synaptotagmin 4. Nat. Struct. Mol. Biol. 2004, 11, 844–849.
4. Sugita, S.; Han, W.; Butz, S.; Lao, Y.; Liu, X.; Ferna, R.; Su, T.C.; Hines, H.; Na, B. Synaptotagmin VII as a plasma membrane Ca(2+) sensor in exocytosis. Neuron 2001, 30, 459–473.
5. Bhalla, A.; Tucker, W.C.; Chapman, E.R. Synaptotagmin Isoforms Couple Distinct Ranges of Ca2+, Ba2+ and Sr2+ Concentration to SNARE-mediated Membrane Fusion. Mol. Biol. Cell 2005, 16, 4755–4764.
6. Li, C.; Ullrich, B.; Zhang, J.Z.; Anderson, R.G.W.; Brose, N.; Südhof, T.C. Ca2+-dependent and -independent activities of neural and non-neural synaptotagmins. Nature 1995, 375, 594–599.
7. Wolfes, A.C.; Dean, C. The diversity of synaptotagmin isoforms. Curr. Opin. Neurobiol. 2020, 63, 198–209.
8. Yoo, E.S.; Yu, J.; Sohn, J.W. Neuroendocrine control of appetite and metabolism. Exp. Mol. Med. 2021, 53, 505–516.
9. Moghadam, P.K.; Jackson, M.B. The Functional Significance of Synaptotagmin Diversity in Neuroendocrine Secretion. Front. Endocrinol. 2013, 4, 124.
10. Von Poser, C.; Ichtchenko, K.; Shao, X.; Rizo, J.; Südhof, T.C. The evolutionary pressure to inactivate: A subclass of synaptotagmins with an amino acid substitution that abolishes Ca2+ binding. J. Biol. Chem. 1997, 272, 14314–14319.
11. Von Poser, C.; Südhof, T.C. Synaptotagmin 13: Structure and expression of a novel synaptotagmin. Eur. J. Cell Biol. 2001, 80, 41–47.
12. Fukuda, M.; Mikoshiba, K. Synaptotagmin-like protein 1-3: A novel family of C-terminal-type tandem C2 proteins. Biochem. Biophys. Res. Commun. 2001, 281, 1226–1233.
13. Willmann, S.J.; Mueller, N.S.; Engert, S.; Sterr, M.; Burtscher, I.; Raducanu, A.; Irmler, M.; Beckers, J.; Sass, S.; Theis, F.J.; et al. The global gene expression profile of the secondary transition during pancreatic development. Mech. Dev.

2016, 139, 51–64.

14. Han, S.; Hong, S.; Lee, D.; Lee, M.H.; Choi, J.S.; Koh, M.J.; Sun, W.; Kim, H.; Lee, H.W. Altered expression of synaptotagmin 13 mRNA in adult mouse brain after contextual fear conditioning. Biochem. Biophys. Res. Commun. 2012, 425, 880–885.
15. Nizzardo, M.; Taiana, M.; Rizzo, F.; Aguila Benitez, J.; Nijssen, J.; Allodi, I.; Melzi, V.; Bresolin, N.; Comi, G.P.; Hedlund, E.; et al. Synaptotagmin 13 is neuroprotective across motor neuron diseases. Acta Neuropathol. 2020, 139, 837–853.
16. Hitz, C.; Wurst, W.; Kühn, R. Conditional brain-specific knockdown of MAPK using Cre/loxP regulated RNA interference. Nucleic Acids Res. 2007, 35, e90.
17. Gronostajski, R.M.; Sadowski, P.D. The FLP recombinase of the Saccharomyces cerevisiae 2 microns plasmid attaches covalently to DNA via a phosphotyrosyl linkage. Mol. Cell. Biol. 1985, 5, 3274–3279.
18. Mittelsteadt, T.; Seifert, G.; Alvárez-Barón, E.; Steinhäuser, C.; Becker, A.J.; Schoch, S. Differential mRNA expression patterns of the synaptotagmin gene family in the rodent brain. J. Comp. Neurol. 2009, 512, 514–528.
19. Watson, C.; Kirkcaldie, M.; Paxinos, G. Techniques for studying the brain. In The Brain, 1st ed.; Academic Press: San Diego, CA, USA; pp. 153–165.
20. Böttcher, A.; Büttner, M.; Tritschler, S.; Sterr, M.; Aliluev, A.; Oppenländer, L.; Burtscher, I.; Sass, S.; Irmler, M.; Beckers, J.; et al. Non-canonical Wnt/PCP signalling regulates intestinal stem cell lineage priming towards enteroendocrine and Paneth cell fates. Nat. Cell Biol. 2021, 23, 23–31.
21. Huang, C.; Walker, E.M.; Dadi, P.K.; Hu, R.; Xu, Y.; Zhang, W.; Sanavia, T.; Mun, J.; Liu, J.; Nair, G.G.; et al. Synaptotagmin 4 Regulates Pancreatic β Cell Maturation by Modulating the Ca2+ Sensitivity of Insulin Secretion Vesicles. Dev. Cell 2018, 45, 347–361.
22. Dolai, S.; Xie, L.; Zhu, D.; Liang, T.; Qin, T.; Xie, H.; Kang, Y.; Chapman, E.R.; Gaisano, H.Y. Synaptotagmin-7 functions to replenish insulin granules for exocytosis in human islet β-cell. Diabetes 2016, 65, 1962–1976.
23. Andersson, S.A.; Olsson, A.H.; Esguerra, J.L.S.; Heimann, E.; Ladenvall, C.; Edlund, A.; Salehi, A.; Taneera, J.; Degerman, E.; Groop, L.; et al. Reduced insulin secretion correlates with decreased expression of exocytotic genes in pancreatic islets from patients with type 2 diabetes. Mol. Cell. Endocrinol. 2012, 364, 36–45.
